Biochemical Journal (2018) **475** 3797–3812
https://doi.org/10.1042/BCJ20180672

Research Article

Polyamines stimulate the CHSY1 synthesis through the unfolding of the RNA G-quadruplex at the 5′-untraslated region

Katsutoshi Yamaguchi[1,*], Kiryu Asakura[1,*], Masataka Imamura[1], Gota Kawai[2], Taiichi Sakamoto[2], Tomomi Furihata[1], Robert J. Linhardt[3], Kazuei Igarashi[1,4], Toshihiko Toida[1] and Kyohei Higashi[1,5]

[1]Department of Clinical and Analytical Biochemistry, Graduate School of Pharmaceutical Sciences, Chiba University, 1-8-1 Inohana, Chuo-ku, Chiba 260-8675, Japan; [2]Department of Life and Environmental Sciences, Chiba Institute of Technology, 2-17-1 Tsudanuma, Narashino, Chiba 275-0016, Japan; [3]Department of Biology, Center for Biotechnology and Interdisciplinary Studies, Rensselaer Polytechnic Institute, 110 8th Street, Troy, NY 12180, U.S.A.; [4]Amine Pharma Research Institute, Innovation Plaza at Chiba University, 1-8-15 Inohana, Chuo-ku, Chiba 260-0856, Japan; [5]Department of Clinical and Analytical Biochemistry, Faculty of Pharmaceutical Sciences, Tokyo University of Science, 2641 Yamazaki, Noda, Chiba 278-8510, Japan

Correspondence: Kyohei Higashi (higase@rs.tus.ac.jp)

Glycosaminoglycans (GAGs), a group of structurally related acidic polysaccharides, are primarily found as glycan moieties of proteoglycans (PGs). Among these, chondroitin sulfate (CS) and dermatan sulfate, side chains of PGs, are widely distributed in animal kingdom and show structural variations, such as sulfation patterns and degree of epimerization, which are responsible for their physiological functions through interactions with growth factors, chemokines and adhesion molecules. However, structural changes in CS, particularly the ratio of 4-*O*-sulfation to 6-*O*-sulfation (4S/6S) and CS chain length that occur during the aging process, are not fully understood. We found that 4S/6S ratio and molecular weight of CS were decreased in polyamine-depleted cells. In addition, decreased levels of chondroitin synthase 1 (CHSY1) and chondroitin 4-*O*-sulfotransferase 2 proteins were also observed on polyamine depletion. Interestingly, the translation initiation of CHSY1 was suppressed by a highly structured sequence (positions −202 to −117 relative to the initiation codon) containing RNA G-quadruplex (G4) structures in 5′-untranslated region. The formation of the G4s was influenced by the neighboring sequences to the G4s and polyamine stimulation of CHSY1 synthesis disappeared when the formation of the G4s was inhibited by site-directed mutagenesis. These results suggest that the destabilization of G4 structures by polyamines stimulates CHSY1 synthesis and, at least in part, contribute to the maturation of CS chains.

Introduction

Glycosaminoglycans (GAGs) including chondroitin sulfate (CS), dermatan sulfate (DS), heparin and heparan sulfate (HS), are linear, sulfated polysaccharides comprised of 50–200 repeating disaccharides of hexosamine and uronic acid, and are the glycan moieties of proteoglycan glycoconjugates [1]. CS consists of a distinctive repeating disaccharide unit [→4)-β-D-GlcA-(1 → 3)-β-D-GalNAc-(1→]$_n$, where GlcA is glucuronic acid and GalNAc is *N*-acetyl-D-galactosamine. Some hydroxyl groups in disaccharide units are replaced by sulfo groups (S) resulting in the diversity of the CS disaccharide units, which include GlcA–GalNAc (O-unit), GlcA–GalNAc (4S) (A-unit), GlcA–GalNAc (6S) (C-unit), GlcA (2S)–GalNAc (6S) (D-unit) and GlcA–GalNAc (4S, 6S) (E-unit) [2–4]. CS biosynthesis is initiated once GalNAc is transferred by CSGalNAcT1 or 2 to the common linkage tetrasaccharide, GlcAβ1–3galactose (Gal)β1–3Galβ1–4xylose (Xyl)β1-*O*-serine in proteoglycans and chain elongation is then catalyzed by the chondroitin synthase (CHSY) 1–3/chondroitin-polymerizing factor (CHPF) heterodimer [3–5]. After synthase-catalyzed polymerization, the majority of the GalNAc residues are

*These authors contributed equally to this work.

Received: 16 August 2018
Revised: 4 October 2018
Accepted: 5 November 2018

Accepted Manuscript online: 6 November 2018
Version of Record published: 6 December 2018

Biochemical Journal (2018) 475 3797–3812
https://doi.org/10.1042/BCJ20180672

4-*O*-sulfated by chondroitin 4-*O*-sulfotransferases (C4ST1, 2 and 3) or 6-*O*-sulfated by chondroitin 6-*O*-sulfotransferases (C6ST1 and 2). In addition, resulting A- or C-unit can be further sulfated by GalNAc 4-sulfate 6-*O*-sulfotransferase (GalNAc4S-6ST) or chondroitin uronyl 2-*O*-sulfotransferase (UST), generating di-sulfated disaccharides, E-unit or D-unit, respectively. A disaccharide unit containing iduronic acid (IdoA) in place of GlcA is commonly found in DS, a stereoisoform of CS that differs in the C-5 configuration of its hexuronic acid moiety [6]. This epimerization of GlcA is catalyzed by dermatan sulfate epimerase (DS-epi1 and DS-epi2) and resulting IdoA-GalNAc (iO-unit) is subsequently sulfated by dermatan 4-*O*-sulfotransferase-1 (D4ST1). Resulting IdoA–GalNAc (4S) (iA-unit) can then be further sulfated by UST, generating IdoA (2S)–GalNAc (4S) (B-unit). Among these disaccharides, di-sulfated disaccharides (B-, D- and E-units) play important roles in CS activities, including cell proliferation, migration, differentiation, cell–cell communications and adhesion through interactions with CS-binding proteins [7]. However, the multiple sulfation of CS/DS by sulfotransferases is intricately regulated at multiple levels in mammals, because most disaccharide units in CS/DS from mammals are A-/iA-units, and di-sulfated disaccharide levels are very low. In addition, the degree of sulfation and C-5 epimerization are tissue-specific and cell type-specific [8–10]. Since mammalian CS/DS exhibits high affinity for growth factors [11], the distribution and number of protein-binding sites containing IdoA and di-sulfated CS disaccharides are believed to be important in mammalian physiology. In fact, alteration of CS/DS structure results in disturbances of the many crucial biological functions of CS (or DS) and can result in various phenotypes associated with genetic disorders of connective tissues [12,13].

There are several reports that structural changes in CS, particularly the ratio of 4-*O*-sulfation to 6-*O*-sulfation (4S/6S), occur during normal embryonic development, during growth, and in aging [14–18]. For example, the 4S/6S ratios of CS (or DS) present in human skin and cartilage decrease from birth to age 20 [15–17]. During development, an increase of 4S/6S ratio is observed in chicken embryo brain [18] and mouse visual cortex [14], suggesting the importance of a change in CS structure, particularly sulfation pattern, in tissue development. While the CS biosynthesis pathway has been elucidated, the mechanism controlling gene expression of CS biosynthetic enzymes during embryogenesis and in aging processes is not well understood.

Polyamines (i.e. putrescine, spermidine and spermine) are present at millimolar concentrations in eukaryotic cells and are essential for the normal cell growth and differentiation [19]. Since polyamines exist mainly as polyamine–RNA complexes (the amount of polyamines bound is ∼2–6.5 mol/100 mol of RNA phosphate) [20], stimulation of cell growth by polyamines is mainly due to the enhancement of the protein synthesis of specific genes related to the cell growth [21]. It has been reported that GAG biosynthesis in rabbit costal chondrocytes increased markedly after the treatment of parathyroid hormone (PTH) through the up-regulation of ornithine decarboxylase (ODC), an initial and rate-limiting enzyme in the polyamine biosynthetic pathway [22]. In addition, GAG biosynthesis, during the differentiation of rabbit costal chondrocytes caused by PTH, depends on an increase in intracellular polyamines [23,24]. However, the detailed mechanism of stimulated GAG biosynthesis by polyamines is not fully understood.

Since tissue polyamine levels decrease during the aging process in animals [25], we examined the correlation between GAG structures and polyamines in human skin and found that polyamine levels correlate with HS levels but not with DS levels [26]. However, biosynthetic pathways both of CS and DS are different, because 4-*O*-sulfation of chondroitin is accomplished by C4ST1, 2 and 3, while 4-*O*-sulfation of dermatan is D4ST1-dependent. For this reason, in the current study, we carefully examined the effect of polyamines on the expression level of CS using 15 different cell lines. We observed a decrease in 4S/6S ratio and molecular weight of CS when intracellular polyamine levels were depleted. In addition, expression levels of CHSY1 and C4ST2 proteins decrease on polyamine depletion. Interestingly, translation initiation of CHSY1 is suppressed by the RNA G-quadruplexes (G4s) present in the 5′-untranslated region (5′-UTR). The formation of these G4s is influenced by the neighboring sequences of the G4 structures and polyamine stimulation of CHSY1 synthesis disappears when the formation of G4s is inhibited by site-directed mutagenesis. These results suggest that destabilization of the G4 structures by polyamines stimulates CHSY1 synthesis and, at least in part, contribute to the maturation of CS chains.

Experimental procedures

Materials

Actinase E was purchased from Kaken Pharmaceutical Co., Ltd (Tokyo, Japan). Chondroitinase ABC (ChaseABC) from *Proteus vulgaris*, heparinase I, heparinase II, heparinase III from *Flavobacterium heparinum* and unsaturated disaccharides of CS (ΔDi-0S, ΔDi-4S, ΔDi-6S, ΔDiUA-2S, ΔDi-diS_E, ΔDi-diS_B, ΔDi-diS_D and

Biochemical Journal (2018) **475** 3797–3812
https://doi.org/10.1042/BCJ20180672

ΔDi-TriS) were purchased from Seikagaku Kogyo Co., Ltd (Tokyo, Japan). The molecular weight standards of dp6 (M_w: 1488), dp10 (M_w: 2480) and dp20 (M_w: 4960) from CS were obtained from Iduron (Manchester, U. K.). α,β,γ,δ-Tetrakis(1-methylpyridinium-4-yl)porphyrin *p*-toluenesulfonate (TmPyP4) was purchased from Tokyo Chemical Industry Co., Ltd (Tokyo, Japan).

Cell culture

CHO-K1, CCF-STTG1, HepG2, HEK293, Caco-2, MCF7 and PANC-1 were purchased from ATCC (Manassas, VA, U.S.A.). ATDC5 was purchased from RIKEN Cell Bank (Ibaraki, Japan). U2OS, HCT116, A549 and Neuro2a were kindly supplied by Dr Murai (The Jikei University School of Medicine, Japan), Dr Fukumoto (Chiba University, Japan), Dr Nakamura (Chiba University, Japan) and Dr Kitagawa (Kobe Pharmaceutical University, Japan), respectively. Cells were cultured in Dulbecco's modified Eagle's medium supplemented with 10% fetal bovine serum (FBS), 100 units ml^{-1} penicillin G and 50 units ml^{-1} streptomycin in an atmosphere of 5% CO_2/95% air at 37°C. A three-fold greater number of cells were cultured in DMEM in the presence of α-difluoromethylornithine (DFMO) for 3 days to make polyamine-depleted cells. The concentration of DFMO used in this study is presented in Supplementary Table S1.

High-performance liquid chromatography of unsaturated disaccharides of CS

Cells (1×10^7) were freeze-dried overnight and treated with actinase E (0.25 mg ml^{-1}) in 400 μl of 50 mM Tris–acetate buffer (pH 8.0) at 45°C for 3 days. Microscale isolation of GAGs was performed as described recently [26]. Briefly, the filtered extracts were purified by a Vivapure Q mini H spin column (Sartorius Stedim Biotech GmbH, Göttingen, Germany) centrifugation, and then columns were washed three times with 450 μl of 0.2 M NaCl. Crude GAGs were then eluted from the column by washing twice with 500 μl of 16% NaCl. The GAGs were precipitated from the supernatant by the addition of four volumes of cold methanol for 16 h at 4°C and were recovered by centrifugation at 11 000×***g*** for 30 min. The whole GAG samples were incubated in the reaction mixture (35 μl) containing 28.6 mM Tris–acetate (pH 8.0) and 50 mIU of Chase ABC for 16 h at 37°C. Depolymerized samples were boiled, and unsaturated disaccharides of CS were collected by Amicon Ultra Centrifugal Filter 30 K device (Merck Millipore, Billerica, MA, U.S.A.).

Disaccharide composition analysis of CS was performed by reversed-phase ion-pairing chromatography with sensitive and specific post-column detection. A gradient was applied at a flow rate of 1.0 ml min^{-1} on Senshu Pak Docosil (4.6 × 150 mm; Senshu Scientific Co., Ltd, Tokyo, Japan) at 60°C. The eluent buffers were as follows: A, 10 mM tetra-*n*-butylammonium hydrogen sulfate in 12% methanol; B, 0.2 M NaCl in buffer A. The gradient program was as follows: 0–10 min (1% B), 10–11 min (1–10% B), 11–30 min (10% B), 30–35 min (10–60% B) and 35–40 min (60% B). Aqueous (0.5% (w/v)) 2-cyanoacetamide solution and 1 M NaOH were added to the eluent at the same flow rates (0.25 ml min^{-1}) by using a double plunger pump. The effluent was monitored fluorometrically (Ex., 346 nm; Em., 410 nm). The expression level of CS was expressed as total amounts of unsaturated disaccharides. Protein contents were determined by the method of Lowry et al. [27]. The composition of unsaturated disaccharides of CS was shown in Supplementary Table S1.

Determination of molecular weight of CS from cultured cells

Molecular weights of CS from cells cultured with or without DFMO were analyzed by size exclusion chromatography. At first, 1×10^7 of HCT116 cells were freeze-dried overnight and treated with actinase E (0.25 mg ml^{-1}) in 400 μl of 50 mM Tris–acetate buffer (pH 8.0) at 45°C for 3 days. Next, 8 mg of CHAPS (final 2.0%) and 192.2 mg of urea (final 8.0 M) were added to solubilize samples completely. After the adjustment of pH to 6.0 in cell lysate using 2.5 M acetic acid, samples were subjected to a Vivapure D mini H spin column (Sartorius Stedim Biotech GmbH, Göttingen, Germany) centrifugation and eluted with 900 μl of 50 mM sodium phosphate buffer (pH 6.0) containing 0.6, 0.8, 1.0 and 1.2 M NaCl in a stepwise manner. The 1.2 M NaCl fraction containing CS and small amount of HS, but not HA, was subjected to β-elimination by the addition of 300 μl of 0.5 M NaOH containing 4% $NaBH_4$ and incubated at 4°C for 16 h. After the β-elimination, sample was neutralized with 1 M HCl. The GAGs, mixed with 8 ml of cold methanol and incubated with for 16 h at 4°C, were recovered by centrifugation at 11 000×***g*** for 30 min at 4°C. The precipitated GAG samples were treated with 1 mIU heparinase I, II and III, respectively, and residual CS chains were collected by Amicon Ultra Centrifugal Filter 3 K device (Merck Millipore, Billerica, MA, U.S.A.) and subjected to gel permeation chromatography (GPC). GPC condition: column, an Asahipak 510 HQ column (7.6 mm, i.d. ×300 mm) (Showa Denko K.K., Tokyo, Japan) and eluted with 10 mM NH_4HCO_3 at a flow rate of 0.3 ml min^{-1}. CS chains were detected by

Biochemical Journal (2018) 475 3797–3812
https://doi.org/10.1042/BCJ20180672

UV at 204 nm. The GPC chromatograms were recorded and analyzed with Chromato-PRO-GPC data processing software (Run Time Instruments, Kanagawa, Japan).

Western blot analysis

Western blot analysis was performed by the method of Nielsen et al. [28] using the Amersham™ ECL Select™ Western Blotting Detection System (GE Healthcare UK Ltd, Buckinghamshire, U.K.). Antibodies used in this study are listed in Supplementary Table S2. Protein levels were quantified by an ImageQuant™ LAS 4000 (GE Healthcare UK Ltd, Buckinghamshire, U.K.) instrument. Protein contents were determined by the method of Lowry et al. [27].

Plasmids

PCR was performed using the primer sets, P1 and P2, and chromosomal DNA isolated from HCT116 cells was used as a template to amplify the 5′-UTR of CHSY1 (494 bp) gene. All primers used for the construction of pCHSY1-EGFP, pCHSY1-EGFP mutants are listed in Supplementary Table S3. The amplified CHSY1 gene containing 5′-UTR and N-terminal coding sequence (CDS) was digested with EcoRI and BamHI, and inserted into the same restriction site of pEGFP-N1 (Takara Bio, Inc., Shiga, Japan). PCR was performed using primers listed in Supplementary Table S3 and pCHSY1(494)-EGFP was used as a template to make pCHSY1-EGFP mutants [pCHSY1 (Δ-494-422)-EGFP, pCHSY1 (Δ-421-314)-EGFP, pCHSY1 (Δ-421-215)-EGFP, pCHSY1 (Δ-421-110)-EGFP]. pCHSY1 (Δ-494-422)-EGFP was used as a pCHSY1 (WT)-EGFP in this study. pCHSY1 (Δ-303-214)-EGFP, pCHSY1 (Δ-202-117)-EGFP, pCHSY1 (Δ-202+60)-EGFP, pCHSY1 (Δ-105+60)-EGFP, pCHSY1 (MUT-186-172)-EGFP, pCHSY1 (MUT-150-138)-EGFP, pCHSY1 (MUT-186-172 and MUT-150-138)-EGFP, pCHSY1 (MUT-184-166)-EGFP, pCHSY1 (MUT-155-134)-EGFP, pCHSY1 (MUT-184-166 and MUT-155-134)-EGFP and pCHSY1 (MUT-145-135)-EGFP were constructed using pCHSY1 (WT)-EGFP as a template and primers were listed in Supplementary Table S3. The plasmid sequences were confirmed by DNA sequence service (Eurofins Genomics K. K., Tokyo, Japan).

Transfection of plasmids

Transfection of plasmids into HeLa cells was performed according to the method of Fukumoto et al. [29] with minor modifications. Briefly, 1 μg of plasmids was mixed with 5 μg of polyethyleneimine (Polysciences, Inc., Warrington, PA, U.S.A.) in 100 μl of buffer [20 mM sodium lactate, 150 mM NaCl (pH 4.0)] and stand for 20 min at room temperature, and then 500 μl of Opti-MEM®I (Thermo Fisher Scientific, Inc., Waltham, MA, U.S.A.) was added. Cells (1.5×10^5 in each well of six well plates) were cultured with or without 5 mM DFMO for 12 h. After changing the medium with a fresh one containing FBS, cells were transfected with 600 μl of plasmid/polyethyleneimine complex in Opti-MEM and cultured in DMEM containing FBS with or without 5 mM DFMO for 8 h. After replacing the culture medium with fresh one, cells were cultured with or without 5 mM DFMO for further 16 h.

Gene knockdown

Silencer® select siRNAs for eIF5A (eukaryotic translation initiation factor 5A), eIF4AI (eukaryotic translation initiation factor 4AI) and CHSY1 were purchased from Thermo Fisher Scientific, Inc. (Waltham, MA, U.S.A.). The following siRNA sequences were used in this study: 5′-r (GGUCCAUCUGGUUGGUAUU)d (TT)-3′ for eIF5A [30] and 5′-r (GCCCAAUCUGGGACUGGGA)d (TT)-3′ for eIF4AI [31]. As for CHSY1, the following siRNA sequences were used: #1, 5′-r (GGAUCCUCCCAGUUUAACA)d (TT)-3′; #2, 5′-r (GCAUCACGUGUAUUUAUAA)d (TT)-3′; #3, 5′-r (GAAUUACGAGCAGAACAAA)d (TT)-3′. As a scrambled control, Silencer select Control No. 1 siRNA (catalog no. 4390843) was used. Transfection of siRNA into HCT116 cells was performed with Lipofectamine RNAiMAX (Thermo Fisher Scientific, Inc., Waltham, MA, U.S.A.) according to the accompanying manual. Briefly, 30 nM siRNA was mixed with Lipofectamine RNAiMAX in 500 μl Opti-MEM and stand for 15 min at room temperature. HCT116 cells (1.5×10^5 cells/2.5 ml) in six well plates were transfected with siRNA/Lipofectamine RNAiMAX complex in Opti-MEM and cultured in DMEM containing FBS with or without 5 mM DFMO for 48 h.

Measurement of mRNA

Total RNA was isolated with the RNeasy Mini Kit (Qiagen GmbH, Hilden, Germany). DNase treatment of RNA samples prior to reverse transcription was performed using RQ1 RNase-Free DNase (Promega, Madison,

Biochemical Journal (2018) **475** 3797–3812
https://doi.org/10.1042/BCJ20180672

WI, U.S.A.). After removal of degraded DNA by the Amicon Ultra-0.5 ml Centrifugal Filters 3K device (Merck Millipore, Billerica, MA, U.S.A.), synthesis of the first-strand cDNA from total RNA was performed using SuperScript™ II Reverse Transcriptase (Thermo Fisher Scientific, Inc., Waltham, MA, U.S.A.) according to the accompanied manual. Quantitative PCR (qPCR) with SYBR Advantage qPCR Premix (Takara Bio Inc., Shiga, Japan) was performed using primers listed in Supplementary Table S3. The transcript levels were calculated by $2^{-\Delta\Delta C_t}$ method. Transcription of the housekeeping gene *GAPDH* was used to normalize data.

Nuclear magnetic resonance and circular dichroism

PQS5 (5′-CCCGCGGCGGCGGCGGCGCUG-3′) and MUT-145-135 (5′-CCCGCAACAACAACAACGCUG-3′) oligonucleotides were obtained from Hokkaido System Science Co. Ltd (Hokkaido, Japan). RNA oligonucleotides were purified by centrifugation with an Amicon Ultra Centrifugal Filter (3000 molecular weight cut off). RNA samples in H_2O were annealed by heating at 90°C for 5 min, followed by snap-cooling on ice. NMR (nuclear magnetic resonance) spectra were recorded at a probe temperature of 283 K (10°C) using DRX-600 spectrometer (Bruker). NMR samples (0.4 ml) contained 10 mM Tris–HCl, pH 7.5, 0.06 mM PQS5 or MUT-145-135 RNA and 5% D_2O. CD (Circular dichroism) spectra were recorded 190–320 nm on a Jasco J-1100 spectropolarimeter using a 0.1 cm path length cuvette at 25°C. Scan speed was 50 nm min^{-1}, and CD samples contain 10 mM Tris–HCl (pH 7.5), 0.1 mM EDTA and 10 μM RNA. After the addition of 50 mM KCl, $MgCl_2$ and/or spermidine was added to the CD samples at the specified concentrations.

Results

Effect of polyamines on the CS structures in cultured cells

Comprehensive analysis of CS expressed in 15 cell types was first performed using HPLC (high-performance liquid chromatography), and expression levels and sulfation patterns of CS were found to be cell type-dependent (Supplementary Table S1). The amount of CS present in CCF-STG1 was the highest (2660 ng mg^{-1} proteins) and Neuro2a was the lowest (1.75 ng mg^{-1} proteins) of the 15 cell types tested. The

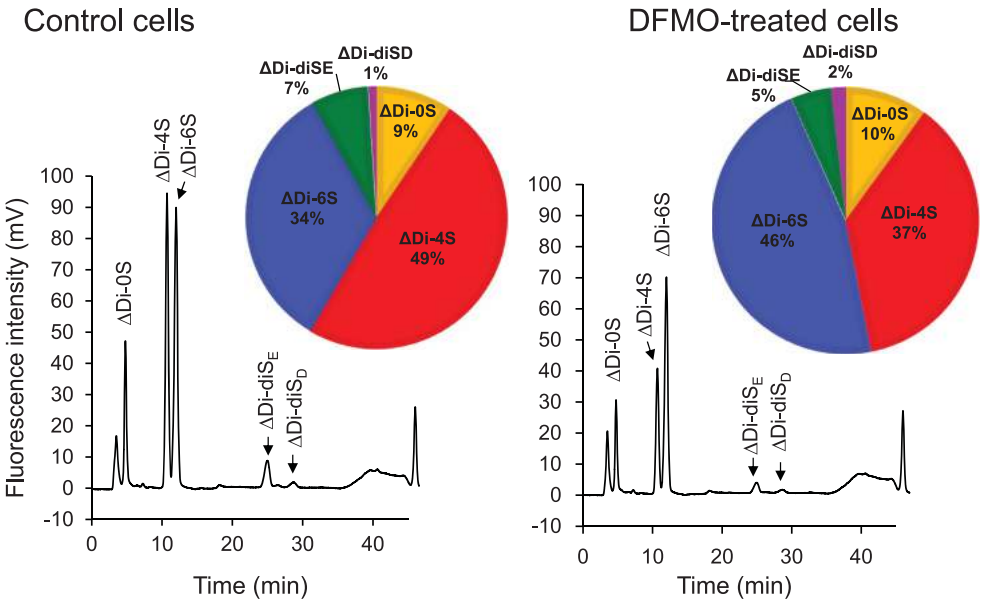

Figure 1. Effect of polyamines on CS structure in HCT116 cells.

Chromatogram and disaccharide compositions of CS in HCT116 cells cultured with or without 5 mM DFMO for 3 days. GAGs containing CS from 1×10^7 cells were treated with 50 mIU of ChaseABC, and resulting unsaturated disaccharides were submitted to HPLC. Note that ΔDi-4S peak was significantly decreased in DFMO-treated HCT116 cells. Detailed expression level and disaccharide composition of CS in HCT116 cells are shown in Supplementary Table S1.

Biochemical Journal (2018) **475** 3797–3812
https://doi.org/10.1042/BCJ20180672

major disaccharide units comprising the CS from 15 cell types could be divided into three groups of sulfation patterns. The O-unit (ΔDi-0S in Supplementary Table S1) was present as a major disaccharide in the CS from U2OS, C2C12 and PANC-1. In contrast, the A-unit (ΔDi-4S) was the predominant disaccharide present in CS from NIH3T3, ATDC5, CHO-K1, CCF-STG1, HeLa, HepG2, HCT116, A549, HEK293, MCF-7 and Neuro2a. The C-unit (ΔDi-6S) was predominant in Caco-2. The E-unit (ΔDi-diS_E) was characteristic of CS from MCF-7, consistent with the observation that an increased percentage of E-unit occurs in breast tissue-derived cell lines [8]. The effect of polyamines on CS structure was next examined using DFMO, an irreversible inhibitor of ODC, the rate-limiting enzyme in polyamine synthesis. Under the cell culture conditions used, the levels of both putrescine and spermidine were negligible as described recently [26], and on exposure to DMFO, the cell numbers decreased by ∼30% within 3 days as compared with control cells. HCT116 cells, producing a CS with substantial amounts of both A- and C-units, showed a significant decrease in ΔDi-4S (A-unit) when intracellular polyamine levels decreased on DFMO treatment (Figure 1). Among the other 15 cell types, the absolute amount and relative proportion of ΔDi-4S (A-unit) decreased on DFMO treatment for the NIH3T3, ATDC5, HCT116, C2C12, A549, HEK293 and PANC-1 cell lines (Supplementary Table S1). In addition, a decrease in the 4S/6S ratio was observed in DFMO-treated ATDC5, HeLa, HepG2, HCT116, C2C12, A549, HEK293, Caco-2, MCF-7 and PANC-1 cell lines (Supplementary Table S1). In NIH3T3, CHO-K1 and Neuro2a, examination of polyamine effect on the 4S/6S ratio could not be calculated because no C-unit (ΔDi-6S) was detected.

Next, the effect of polyamines on CS molecular weight was examined using GPC-HPLC analysis (Supplementary Figure S1). The chromatogram of CS derived from HCT116 control cells shows high polydispersity with a number average molecular weight (M_N) of 7.6 kDa and weight average molecular weight (M_W) of 33 kDa. Polyamine depletion resulted in a decrease in CS molecular weight to M_N of 4.2 kDa and M_W of 21 kDa. These results suggest that CS structure, both chain length and 4S/6S ratio, can be modulated by intracellular polyamine levels.

Polyamines stimulate the syntheses of CHSY1 and C4ST2 in HCT116 cells

CS chain elongation is catalyzed by the CHSY 1–3/CHPF heterodimer and 4-*O*-sulfation is catalyzed through the action of chondroitin 4-*O*-sulfotransferases (C4ST1, 2 and 3) [3,4]. Because both the 4-*O*-sulfation and molecular weight of CS were decreased in DFMO-treated HCT116 cells (Figure 1 and Supplementary Figure S1), we looked at the expression levels of these CS biosynthetic enzymes using Western blotting. The expression levels of both C4ST2 and CHSY1 proteins also decreased in DFMO-treated HCT116 cells (Figure 2A). Next, the effect of polyamines on the transcription level of the genes encoding C4ST2 and CHSY1 was examined. As shown in Figure 2B, the level of mRNA encoding C4ST2 was decreased in DFMO-treated HCT116 cells, while the level of mRNA encoding CHSY1 in DFMO-treated cells was nearly identical with control cells. These results suggest that CHSY1 synthesis is enhanced by polyamines at the translational level, while C4ST2 is stimulated at the transcriptional level.

Additional biochemical studies on polyamine stimulation of CHSY1 were next performed. When the polyamine spermidine (SPD) was added to rescue DFMO-treated cells, cell growth (data not shown) and the level of CHSY1 expression could be substantially recovered (Figure 2C). It is well established that eIF5A, containing hypusine derived from spermidine, is involved in cell growth [32]. Thus, we examined whether hypusinated eIF5A was related to CHSY1 biosynthesis or not. While the level of eIF5A protein clearly decreased when siRNA [30] was transfected, the level of CHSY1 was comparable to control cells (Figure 2D). These results suggest that polyamines directly stimulate the protein synthesis of CHSY1.

Polyamine stimulation of CHSY1 synthesis is caused at the translation initiation step

A plasmid containing 5′-UTR and N-terminal amino acid CDS of *CHSY1* gene fused to the *EGFP* (enhanced green fluorescent protein) gene was next constructed to elucidate the molecular mechanism of polyamine stimulation of CHSY1 biosynthesis (Figure 3A). It should be noted that 5′-UTR of the mRNA encoding *CHSY1* is 421 nucleotides long and has high GC content (86%), and there are two types of AUG initiation codons in the *CHSY1* gene and *EGFP* gene in the open reading frame (ORF). Translational fusion containing two in-frame AUG codons, an upstream AUG predicted to initiate the synthesis of CHSY1–EGFP fusion protein and a downstream AUG predicted to initiate the synthesis of EGFP protein, so that 1st (CHSY1–EGFP fusion protein:

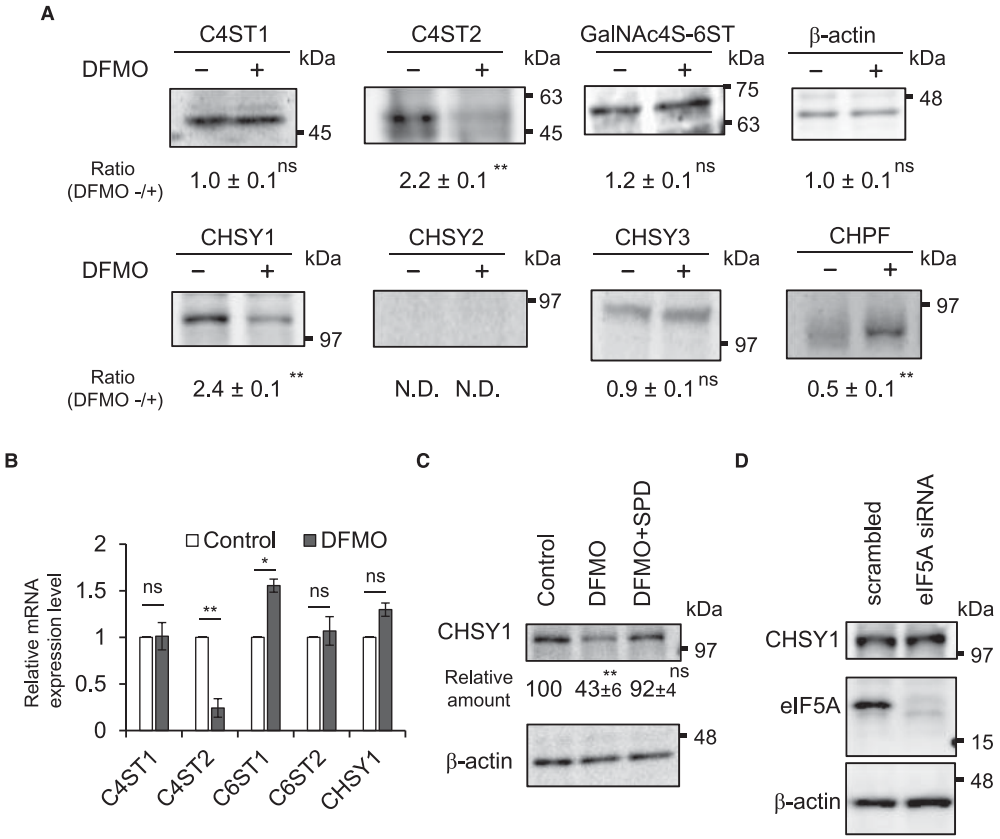

Figure 2. Polyamines stimulate the synthesis of CHSY1 and C4ST2.

(**A**) Effect of polyamine depletion on the expression level of glycosyltransferases (CHSY1-3, CHPF) and sulfotransferases (C4ST1, 2 and GalNAc4S-6ST) of CS in HCT116 cells. For Western blotting of each proteins and β-actin, 20 μg (CHSY1-3, CHPF, C4ST1, 2 and GalNAc4S-6ST) or 5 μg (β-actin) of protein of whole cell lysate, prepared from cells cultured with or without 5 mM DFMO for 3 days, was used. Data are expressed as the mean ± s.e.m. ($n = 3$) of three independent experiments. (**B**) Effect of polyamine depletion on the expression level of mRNAs of glycosyltransferases and sulfotransferases in HCT116 cells. Cells were cultured with or without 5 mM DFMO for 3 days, and RNA was extracted and converted to cDNA for real-time PCR analysis. Data were calculated using by the $2^{-\Delta\Delta C_t}$ method. Transcription of the housekeeping gene *GAPDH* was used to normalize data. Data are expressed as the mean ± s.e.m. ($n = 3$) of three independent experiments. Primers listed are described in Supplementary Table S3. (**C**) Effects of 25 μM SPD on the expression level of CHSY1 in DFMO-treated HCT116 cells. To avoid the degradation of SPD, 1 mM aminoguanidine, an inhibitor of serum amine oxidase, was added together with SPD in culture medium for 3 days. Data are expressed as the mean ± s.e.m. ($n = 3$) of three independent experiments. (**D**) Effect of eIF5A knockdown on the expression of CHSY1 protein in HCT116 cells. Transfection of siRNA [30] for eIF5A and Silencer select Control No.1 siRNA was performed as described under 'Experimental procedures'. Note that the CHSY1 expression was maintained despite an inhibition of the synthesis of eIF5A protein. For detection of the eIF5A protein, 20 μg of protein (whole cell lysate) was used. Data are expressed as the mean ± s.e.m. ($n = 3$) of three independent experiments. $^{**}P < 0.01$, $0.01 < {}^{*}P < 0.05$, ns, not significant were determined by two-tailed unpaired Student's *t*-test.

29 kDa) and 2nd (EGFP protein: 27 kDa) products would be produced. Thus, *CHSY1*–EGFP fusion gene was transiently transformed into HeLa cells, and the effect of polyamines on the synthesis of CHSY1–EGFP protein was examined using anti-EGFP antibody. Although the first ATG triplet in the *CHSY1* gene was not in poor context (GCGGGCATGG), 1st and 2nd AUG products were detected and the both proteins were decreased in DFMO-treated HeLa cells (Figure 3B). In contrast, the expression level of CHSY1–EGFP mRNA was nearly equal in cells cultured with or without DFMO (Figure 3C). These results indicate that polyamine stimulation of CHSY1 synthesis is caused at the translation initiation step.

Biochemical Journal (2018) **475** 3797–3812
https://doi.org/10.1042/BCJ20180672

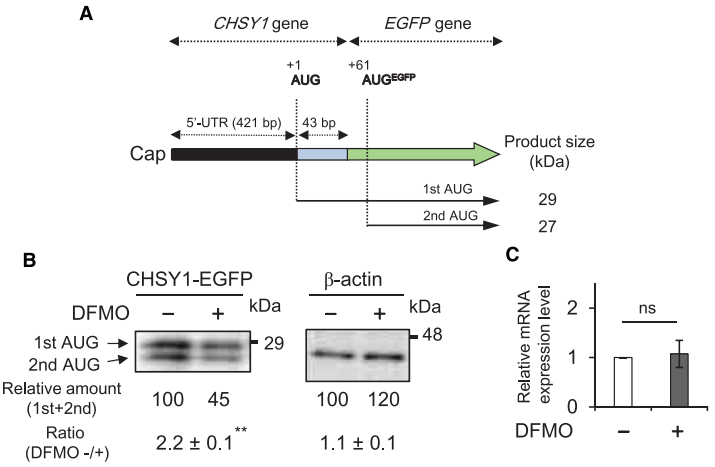

Figure 3. Polyamine stimulation of CHSY1 synthesis is caused at the translation initiation step.

(**A**) Structure of CHSY1–EGFP fusion genes. CHSY1–EGFP fusion protein (29 kDa) and EGFP protein (27 kDa) can be produced by individual AUG codons in CHSY1–EGFP fusion gene. (**B**) Effect of polyamine depletion on the expression levels of 1st and 2nd AUG products in HeLa cells. HeLa cells, but not HCT116 cells, were used in this experiment, because HCT116 cells are highly sensitive to polyethyleneimine exposure, leading to cell aggregation and cell death [29]. HeLa cells (1.5×10^5 cells) cultured with or without 5 mM DFMO for 12 h were treated with plasmid mixture containing 1 μg of pCHSY1-EGFP and 5 μg of polyethyleneimine, and cultured with or without 5 mM DFMO for 8 h. After replacing the culture medium with fresh one, cells were cultured with or without 5 mM DFMO for further 16 h. For Western blotting, 40 μg of protein was used to detect the 1st and 2nd AUG products. Data are expressed as the mean ± s.e.m. ($n = 3$) of three independent experiments. (**C**) Effect of polyamine depletion on the expression level of CHSY1–EGFP mRNA. Transfection of plasmid and real-time PCR were performed as described above. Transcription of the housekeeping gene *GAPDH* was used to normalize data. Data are expressed as the mean ± s.e.m. ($n = 3$) of three independent experiments. $^{**}P < 0.01$, ns, not significant were determined by two-tailed unpaired Student's *t*-test.

5′-UTR sequence at positions −202 to −117 is important for the polyamine stimulation of CHSY1 synthesis

The effect of chain length of 5′-UTR on the polyamine stimulation of CHSY1 was examined using three deletion mutants of pCHSY1 (Δ-421 to -314, relative to the A of AUG codon, which is designated +1)-EGFP, (Δ-421-215) and (Δ-421-110) (Figure 4A). The expression levels of 1st and 2nd AUG products were significantly increased as 5′-UTR length was shortened and the degree of polyamine stimulation was reduced from 2.2-fold to 1.1-fold, despite no change at the mRNA level (Figure 4B,C). Next, four types of deletion experiments pCHSY1 (Δ-105+60)-EGFP, (Δ-202-117), (Δ-202+60) and (Δ-303-214) were constructed to identify the 5′-UTR sequence required for the polyamine stimulation (Figure 4D). When deletion mutants, pCHSY1 (Δ-202-117)-EGFP or (Δ-202+60), were transfected into HeLa cells, the expression levels of resulting 1st + 2nd AUG products from pCHSY1 (Δ-202-117)-EGFP and 1st AUG product from pCHSY1 (Δ-202+60)-EGFP were significantly increased, and polyamine stimulation disappeared despite a lack of change at the mRNA level (Figure 4C,E). In contrast, when deletion mutants of pCHSY1 (Δ-105+60)-EGFP or (Δ-303-214) were used, expression levels and polyamine stimulations of 1st AUG product from pCHSY1 (Δ-105+60)-EGFP and 1st + 2nd products from pCHSY1 (Δ-303-214)-EGFP were unchanged (Figure 4E). These results suggest that 5′-UTR sequence at positions −202 to −117 is important for the polyamine stimulation of CHSY1 synthesis.

G4 structure at positions −145 to −135 in 5′-UTR regulates the CHSY1 synthesis

G4s are guanine-rich nucleic acid structures composed of stacked planar G-quartet motifs that form Hoogsteen hydrogen bonding between guanine molecules [33–35]. Monovalent cations, especially potassium ion, can stabilize G4 structures by intercalation into the central core of a G-tetrad [33]. G4 structures in 5′- and

Biochemical Journal (2018) **475** 3797–3812
https://doi.org/10.1042/BCJ20180672

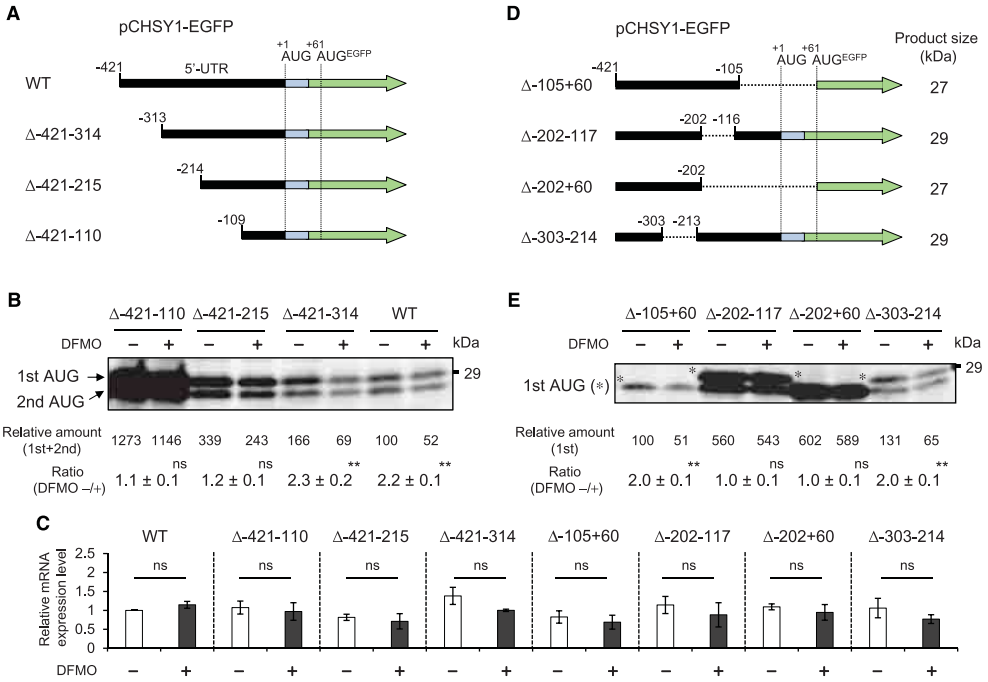

Figure 4. Effect of 5′-UTR deletion on the polyamine stimulation of CHSY1 synthesis.

(**A** and **D**) Structures of deletion mutants of 5′-UTR in CHSY1–EGFP fusion genes. (**B** and **E**) Effect of 5′-UTR deletion on the expression levels of 1st and 2nd AUG products in HeLa cells. Note that deletion mutants of CHSY1 (Δ-105+60) and (Δ-202+60) EGFP protein is only produced because of the deletion of N-terminal CDS in CHSY1 gene. For detection of the 1st and 2nd AUG products, 40 μg of protein (whole cell lysate) was used. Ratios (5 mM DFMO –/+) of 1st and 2nd AUG products in (**B**) and 1st AUG product (*) in (**C**) are expressed as the mean ± s.e.m. ($n = 3$) of three independent experiments. (**C**) Effect of 5′-UTR deletion on the expression level of CHSY1–EGFP fusion mRNAs in HeLa cells. Transfection of plasmids and real-time PCR were performed as described in Figure 2. Transcription of the housekeeping gene *GAPDH* was used to normalize data. Data are expressed as the mean ± s.e.m. ($n = 3$) of three independent experiments. $^{**}P < 0.01$, ns, not significant were determined by two-tailed unpaired Student's *t*-test.

3′-untranslated regions (5′- and 3′-UTRs) and ORF have been found in specific genes, and physiological functions of these were understood to be repression of cap-dependent translation [34]. In fact, most of G4s in the 5′-UTRs repress cap-dependent translation but not transcription by ∼50–80% [36–41]. The potential G4 motif is commonly described as 5′-G_x-$N_{(1-7)}$-G_x-$N_{(1-7)}$-G_x-$N_{(1-7)}$-G_x-3′, where x is 3–6 and N corresponds to any nucleotide (A, G, C, U); however, G4 folding is influenced by neighboring sequences and their trans-acting proteins [34,35,42]. Thus, the stable form causes ribosome arrest and their unfolded state allows ribosome scanning at the 5′-UTR [34,35]. We next looked for the RNA G4 motifs in 5′-UTR by the quadruplex-forming G-rich sequences (QGRS) Mapper (http://bioinformatics.ramapo.edu/QGRS/index.php), and 10 variants, composed of 19–29 nucleotides, were predicted (Supplementary Figure S2). Among these, three putative quadruplex sequences (PQSs) 3–5 are found in 5′-UTR sequence at positions −202 to −117, where polyamine stimulation of CHSY1 synthesis is required. In particular, the 12-nucleotide $(CGG)_4$ sequence corresponding to PQS5 at the positions −145 to −135 is consistent with the G4 structure as recently reported (Supplementary Figure S2) [43]. Thus, analysis of UV melting curves was performed using synthetic oligonucleotides, PQS5 (WT) (5′-CCCGCGGCGGCGGCGGCGCUG-3′) and MUT-145-135 (5′-CCCGCAACAACAACAACGCUG-3′), to confirm G4 structure in 5′-UTR sequence at positions −145 to −135. As shown in Supplementary Figure S3, the melting temperature (T_m) of PQS5 RNA in the presence or absence of 50 mM KCl was higher than 70°C, while the T_m of MUT-145-135 RNA could not be acquired. These results suggest that PQS5 RNA, but not MUT-145-135, can form a structured RNA. NMR spectroscopy is a powerful tool to judge the existence of G4

Biochemical Journal (2018) **475** 3797–3812
https://doi.org/10.1042/BCJ20180672

structure in RNA. Imino proton peaks from 12 to 15 ppm are characteristic of Watson-Crick base pairs, whereas those from 10 to 12 ppm are characteristic of Hoogsteen base pairs of G-quartet formation [44,45]. As shown in Figure 5A, imino proton peaks from Watson-Crick and G-quartet base pairs were observed in PQS5 (WT) RNA but not in MUT-145-135 RNA. In addition, peaks ∼10.5 ppm corresponding to the G-quartet base pairs in PQS5 RNA were stabilized by the addition of 50 mM KCl. This result strongly suggests that PQS5 can fold as a G4 structure.

TmPyP4, a specific intercalator of G4 structures, has been used for the characterization of G4 structures in DNA and RNA. TmPyP4 can suppress the c-MYC transcription activation through stabilization of DNA G4 structure [46], and TmPyP4 can enhance translation by unfolding the RNA G4 structure in MT3-MMP mRNA

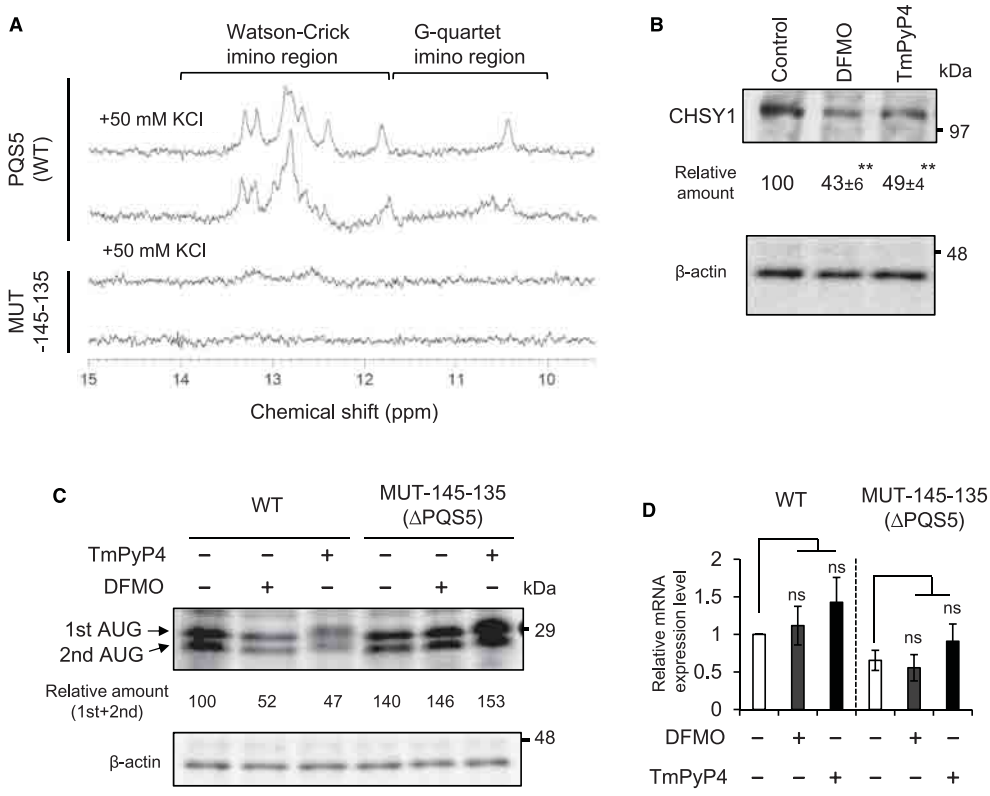

Figure 5. Identification of the G-quadruplex structure in 5′-UTR.

(**A**) Imino region of the ^{1}H-NMR spectra of PQS5 and MUT-145-135 RNA. Spectra were recorded at 10°C in 5% D_2O in the presence or absence of 50 mM KCl. (**B**) Effect of DFMO (5 mM) or TmPyP4 (10 μM) on the expression level of CHSY1 protein in HCT116 cells cultured for 3 days. For detection of the CHSY1 and β-actin proteins, 20 μg and 5 μg of protein (whole cell lysate) were used, respectively. Data are expressed as the mean ± s.e.m. ($n = 3$) of three independent experiments. (**C**) Effect of TmPyP4 (100 μM) on the expression level of 1st and 2nd AUG products from pCHSY1(MUT-145-135)-EGFP. HeLa cells (1.5×10^5 cells) cultured for 12 h were treated with plasmid mixture containing 1 μg of pCHSY1-EGFP and 5 μg of polyethyleneimine, and cultured for 8 h. After replacing the culture medium, cells were cultured with 100 μM TmPyP4 for further 16 h. DFMO treatment was performed as described in Figure 3. For detection of the 1st and 2nd AUG products from *CHSY1–EGFP* fusion gene, 20 μg of proteins (whole cell lysate) was used. Experiments were repeated in triplicate with reproducible results. (**D**) Effect of TmPyP4 (100 μM) on the expression level of CHSY1–EGFP fusion mRNAs in HeLa cells. Transfection of plasmids and real-time PCR were performed as described in Figure 3. Transcription of the housekeeping gene *GAPDH* was used to normalize data. Data are expressed as the mean ± s.e.m. ($n = 3$) of three independent experiments. ** < 0.01, ns, not significant were determined by two-tailed unpaired Student's *t*-test.

[47]. A stabilizing or a destabilizing effect by TmPyP4 depends on the G4 structure (or G4 sequence) [35]. If G4 structure is formed in CHSY1 mRNA expressed in cells, then TmPyP4 treatment influences the CHSY1 synthesis at the translational level. Thus, the effect of TmPyP4 on the expression of CHSY1 protein was examined. When 10 μM of TmPyP4 was treated to HCT116 cells, expression of CHSY1 protein was significantly decreased (Figure 5B). This result suggests that G4 structure existed in CHSY1 mRNA in HCT116 cells and that translation initiation, during the CHSY1 synthesis, might be inhibited by TmPyP4 through the stabilization of G4 structure in CHSY1 mRNA. Next, the effect of TmPyP4 (100 μM) on the expression level of 1st and 2nd AUG products from pCHSY1 (MUT-145-135)-EGFP was examined to determine the G4 structure at positions −145 to −135 in 5′-UTR. As a result, while expression levels of 1st and 2nd AUG products from pCHSY1 (MUT-145-135)-EGFP were slightly increased compared with pCHSY1 (WT)-EGFP, susceptibilities of DFMO and TmPyP4 were diminished (Figure 5C). Levels of mRNAs from pCHSY1 (WT)-EGFP and (MUT-145-135) were not significantly changed by DFMO or TmPyP4 (Figure 5D). These results indicate that G4 structure at positions −145 to −135 in 5′-UTR regulates CHSY1 synthesis in cells and that polyamines or trans-acting proteins whose expression levels might be regulated by polyamines unfold G4 structure.

CD spectroscopy was performed to examine the effect of polyamines on the folding of the G4 structure. The CD spectrum of PQS5 oligonucleotide, but not MUT-145-135, showed a positive peak at 263 nm, a negative peak at 241 nm and an intense negative peak at 214 nm, suggesting the folding of the G4 structure (Supplementary Figure S4). When the SPD was added to the PQS5 oligonucleotides, no significant change in the CD spectrum of G4 structure was observed (Supplementary Figure S4A). Taken together, these results suggest that CHSY1 synthesis is negatively regulated by G4 structure located at the position −145 to −135, and polyamines can indirectly affect this G4 structure.

Formation of G4 structures depends on the neighboring sequence

We have recently reported that the protein synthesis of EXT2 was negatively regulated by miRNA let-7b and that the interaction of let-7b and EXT2 mRNA was directly inhibited by the polyamines [26]. Similarity with miRNA sequences, identified in the −202 to −117 positions (Figure 4E), was searched using miRBase (http://www.mirbase.org), and the possible binding sites of miR-1225-3p and miR-6724-5p were predicted (Supplementary Figure S5). Thus, two potential target sites were mutated to disrupt the base-pairing interaction with miR-1225-3p or miR-6724-5p (Figure 6A,B). The expression levels of 1st and 2nd AUG products expressed from pCHSY1 (MUT-186-172)-EGFP or (MUT-150-138) were significantly increased, and polyamine stimulation had disappeared despite an unchanged level of mRNAs (Figure 6C,D). However, perfect base pairing of miRNA/mRNA in CHSY1 (MUT-184-166)-EGFP and (MUT-155-134) also exhibited the increased levels of 1st and 2nd AUG products and resulted in the disappearance of polyamine stimulation (Figure 6C,D). These results strongly suggest that CHSY1 translation was negatively regulated by G4 structure but not by miR-1225-3p and miR-6724-5p. It is noteworthy that the mutated residues in pCHSY1(MUT-186-172)-EGFP and (MUT-184-166) are far from PQS5 (G4 structure) (Figure 6A). However, the increased expression level of their proteins and the disappearance of the polyamine stimulation were observed (Figure 6C). This result also suggests that the formation of G4 structure is influenced by the neighboring sequence. Thus, the effect of mutations on the formation of G4 structure was investigated by monitoring the susceptibility of the synthesis of 1st and 2nd AUG products to TmPyP4 (Figure 7 and Supplementary Figure S6). It should be noted that the expression levels of 1st and 2nd AUG products from CHSY1-EGFP mutants were higher than it was from wild type despite an unchanged level of mRNA (Figure 7). As expected, the susceptibility of the synthesis of 1st and 2nd AUG products to TmPyP4 completely disappeared when the PQS3-5 deletion mutant of pCHSY1 (MUT-184-166 and MUT-155-134: ΔPQS3+4+5)-EGFP was used (Figure 7A). Interestingly, different susceptibilities of TmPyP4 were observed for the PQS5 mutants. For example, susceptibility of TmPyP4 was diminished when pCHSY1 (MUT-155-134: ΔPQS4+5)-EGFP was transfected (Figure 7A). In contrast, susceptibility of TmPyP4 was retained when pCHSY1 (MUT-150-138: ΔPQS5)-EGFP and (MUT-186-172 and MUT-150-138: ΔPQS3+5) were transfected (Figure 7A). These results suggest that PQS4 may function as G4 structure as well as PQS5. Importantly, PQS3-deletion mutants including (MUT-186-172) and (MUT-184-166) exhibited the increased levels of 1st and 2nd AUG products (1.8-fold), and a strong inhibition of protein synthesis by TmPyP4 treatment was observed (Figure 7A). These results strongly suggest that PQS4 and 5 motifs in PQS3-deletion mutants are unable to form G4 structures and stabilization of G4 structures is required for TmPyP4 treatment. Based on these observations, we conclude that formation of G4 structures depended on the

Biochemical Journal (2018) **475** 3797–3812
https://doi.org/10.1042/BCJ20180672

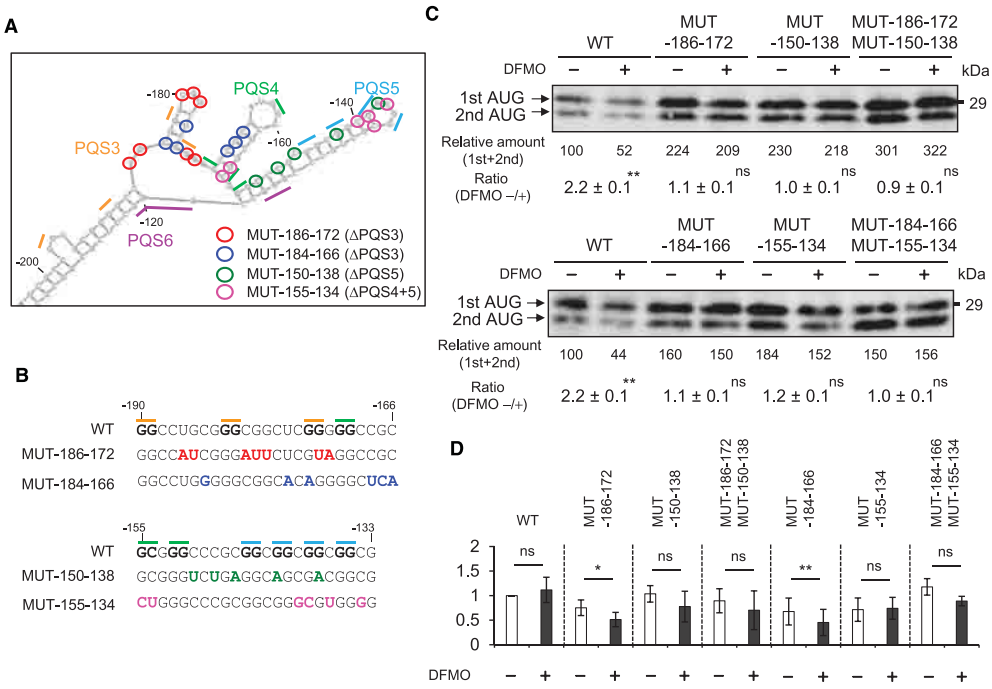

Figure 6. Mutations of PQS3-5 in 5′-UTR afford the increased level of 1st and 2nd AUG products and disappearance of the polyamine stimulation.

(**A**) Position of PQS3-5 and mutated nucleotides in 5′-UTR of CHSY1 mRNA. Possible secondary structure of PQS3-5 in Supplementary Figure S2 is expanded, and mutated nucleotides are circled. (**B**) Sequence of PQS3-5 and their mutants in CHSY1–EGFP fusion gene. Sequences of miR-1225-3p and miR-6724-5p are shown in Supplementary Figure S5. (**C**) Effect of mutations in PQS3-5 on the expression level of 1st and 2nd AUG products in HeLa cells cultured with or without of 5 mM DFMO. Transfection of plasmids and DFMO treatment were performed as described in Figure 3. Forty μg of proteins (whole cell lysate) was used. Data are expressed as the mean ± s.e.m. ($n = 3$) of three independent experiments. (**D**) Effect of mutations in PQS3-5 on the expression level of CHSY1-EGFP fusion mRNAs in HeLa cells. Transfection of plasmids and real-time PCR were performed as described in Figure 3. Transcription of the housekeeping gene *GAPDH* was used to normalize data. Data are expressed as the mean ± s.e.m. ($n = 3$) of three independent experiments. $^{**}P < 0.01$, $0.01 < {}^{*}P < 0.05$, ns, not significant were determined by two-tailed unpaired Student's *t*-test.

neighboring sequence and that the destabilization of their structures by polyamines results in the stimulation of translation initiation of CHSY1 synthesis.

Discussion

Polyamines exist mainly as polyamine–RNA complexes in *Escherichia coli*, bovine lymphocytes and rat liver, and the expression levels of some genes are enhanced by polyamines at the level of translation [21]. We proposed that a set of genes, whose expression is enhanced by polyamines at the level of translation, can be referred to as a 'polyamine modulon' [19,21]. We have recently reported that AUG initiation codon recognition, during translation initiation of EXT2, is repressed by RNA-induced silencing complex containing miRNA let-7b and that the interaction between let-7b and EXT2 mRNA is directly inhibited by polyamines, resulting in the stimulation of EXT2 synthesis at the translational level [26]. In this study, CHSY1 gene was discovered to be a new member of polyamine modulon with a unique stimulation mechanism. We found that translational initiation of the gene responsible for CHSY1 biosynthesis was suppressed by G4 structure in 5′-UTR sequence at positions −145 to −135 (Figure 5C). The destabilization of these G4 structures by polyamines results in the stimulation of translation initiation of CHSY1 synthesis (Figures 5C and 6C). This idea underlies the

Biochemical Journal (2018) **475** 3797–3812
https://doi.org/10.1042/BCJ20180672

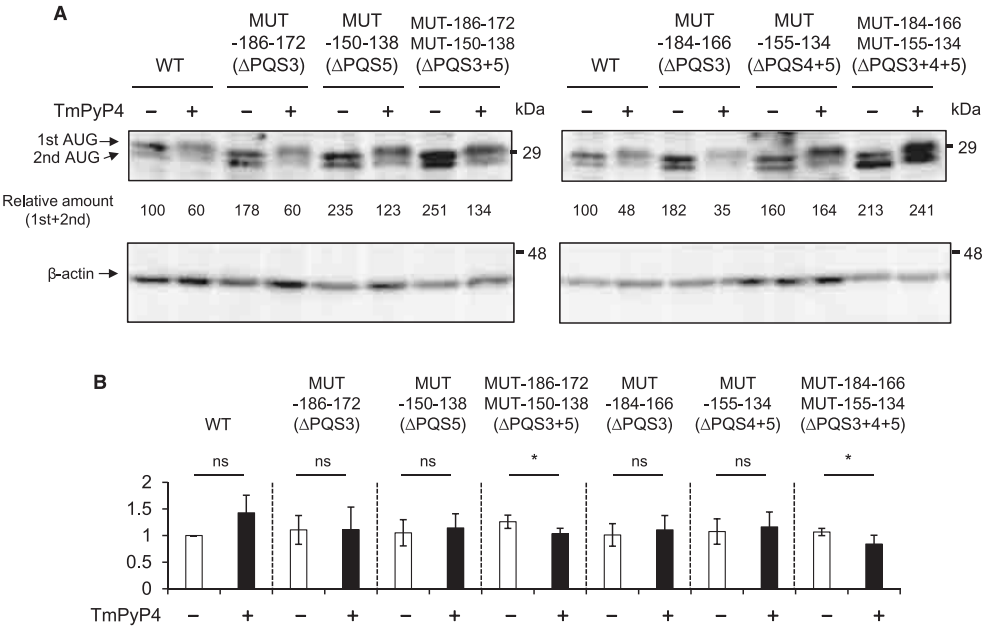

Figure 7. G4 formations are influenced by the neighboring sequence.

(**A**) Effect of TmPyP4 (100 μM) on the expression levels of 1st and 2nd AUG products from PQS3-5 mutants in HeLa cells. Transfection and TmPyP4 treatment were performed as described in Figure 5C. Forty μg of proteins (whole cell lysate) was used. Experiments were repeated in triplicate with reproducible results. (**B**) Effect of TmPyP4 (100 μM) on the expression level of CHSY1–EGFP fusion mRNA from PQS3–5 mutants in HeLa cells. Transfection of plasmids and real-time PCR were performed as described in Figure 3. Transcription of the housekeeping gene *GAPDH* was used to normalize data. Data are expressed as the mean ± s.e.m. ($n = 3$) of three independent experiments. $0.01 < {}^{*}P < 0.05$, ns, not significant were determined by two-tailed unpaired Student's *t*-test.

understanding that stable form of G4s causes the ribosome arrest and their unfolded state allows ribosome scanning at the 5′-UTR [33–35].

Recently, several kinds of G4-binding proteins were identified by pull-down assays and mass spectrometry [48]. Although strong interaction between binding proteins and G4 structures was reported, the physiological role of these binding proteins in the translation of mRNAs having G4 structure remains elusive. A few proteins, including eIF4A, DDX21, CNBP and DHX36, were found to be necessary for the efficient translation of a subset of mRNAs with G4 structures [43,49–51]. DDX21, CNBP and DHX36 can unfold G4s presented in coding sequence (or 3′-UTR), while eIF4A can unfold G4s at the 5′-UTR. Therefore, the effect of eIF4A on the expression level of CHSY1 protein was examined; however, expression level of CHSY1 was unchanged in eIF4A-knockdown cells (Supplementary Figure S7). Because it was reported that CHSY1 synthesis was not influenced by silvestrol [43], an inhibitor of eIF4A, we judged that formation of the G4 structures in 5′-UTR of CHSY1 mRNA was not influenced by eIF4A. Considering that most polyamines (i.e. spermidine and spermine) exist mainly as polyamine–RNA complexes [19,21], we suggest that structural change of mRNA at positions −202 to −117 by polyamines can destabilize, at least in part, the G4s structures, stimulating the translation initiation of CHSY1 synthesis. Because polyamines cannot unfold RNA G4 structure (PQS5 oligonucleotides: 21 mer) directly (Supplementary Figure S4A), experiments are now in progress to clarify the destabilization of G4 structures by polyamines using mRNA at positions −202 to −117.

The present study suggests that stimulation in CHSY1 and C4ST2 synthesis by polyamines cause, at least in part, the level of CS 4-*O*-sulfation and chain polymerization to increase in HCT116 cells. These observations are consistent with the data that GalNAcT-II and GlcAT-II activities are highest on heterodimer formation in

Biochemical Journal (2018) **475** 3797–3812
https://doi.org/10.1042/BCJ20180672

combination with CHSY1 [52], and 4-*O*-sulfation of non-reducing terminal GalNAc-linkage pentasaccharide by C4ST-2 is critical for the initiation of chain elongation of CS [53]. In fact, expression level and the degree of sulfation of CS were significantly decreased in CHSY1-knockdown cells (Supplementary Figure S8). The difference in CS expression level between siRNA-transfected cell (31.4 ng/mg dry weight) and DFMO-treated cells (93.8 ng/mg dry weight) might be explained that the increased level of CHPF by the polyamine depletion compensated CS synthesis (Figure 2A and Supplementary Table S1). As for polyamine stimulation of C4ST2 synthesis, we identified a putative transcription factor modulated by polyamines at the level of translation. Experiments are now in progress to elucidate the stimulation mechanism of the synthesis of putative transcription factor by polyamines.

It is likely that 4S/6S ratio of CS is intricately and strictly regulated by other sulfotransferases. For example, the ratio of C-unit (ΔDi-6S) is significantly increased in DFMO-treated HepG2 and HEK293 cells (Supplementary Table S1). In addition, expression levels of C6ST1 mRNA and CHPF protein were increased in DFMO-treated HCT116 cells (Figure 2A,B). Because expression levels of CHSY1 and C4ST2 depend on the cell types (data not shown), increased expression levels of C6ST1 and CHPF proteins in DFMO-treated cells might cause a decrease of 4S/6S ratio when other cell types were used. In fact, a significant decrease of C6ST activities, along with the reduction of 4S/6S ratio of CS, during chicken embryo brain development has been reported [18]. Further experiments are required to more fully elucidate the regulation of 4S/6S ratio.

In conclusion, a decrease in 4S/6S ratio and molecular weight of CS were observed in polyamine-depleted HCT116 cells. In addition, decreased levels of CHSY1 and C4ST2 proteins on polyamine depletion were also observed. The translational initiation of CHSY1 was suppressed by G4 structure in −145 to −135 regions of 5′-UTR. The formation of G4 structures depends on the sequence context surrounding G4 structures, and the translation initiation was recovered when its formation was impaired by site-directed mutagenesis or in the presence of polyamines. These results suggest that destabilization of G4 structures by polyamines results in the stimulation of CHSY1 synthesis and, at least in part, contribute to the maturation of CS chains.

Abbreviations

4S/6S, 4-*O*-sulfation to 6-*O*-sulfation; 5′-UTR, 5′-untranslated region; C4ST, chondroitin 4-*O*-sulfotransferase; C6ST, chondroitin 6-*O*-sulfotransferase; CD, circular dichroism; CDS, coding sequence; ChaseABC, chondroitinase ABC; CHPF, chondroitin-polymerizing factor; CHSY, chondroitin synthase; CS, chondroitin sulfate; D4ST1, dermatan 4-*O*-sulfotransferase-1; DFMO, α-difluoromethylornithine; DS, dermatan sulfate; DS-epi, dermatan sulfate epimerase; EGFP, enhanced green fluorescent protein; eIF4AI, eukaryotic translation initiation factor 4AI; eIF5A, eukaryotic translation initiation factor 5A; G4s, G-quadruplexes; GAGs, glycosaminoglycans; Gal, galactose; GalNAc 4S-6ST, GalNAc 4-sulfate 6-*O*-sulfotransferase; GalNAc, *N*-acetyl-$_D$-galactosamine; GlcA, glucuronic acid; GPC, gel permeation chromatography; HPLC, high-performance liquid chromatography; HS, heparan sulfate; IdoA, iduronic acid; NMR, nuclear magnetic resonance; ODC, ornithine decarboxylase; ORF, open reading frame; PGs, proteoglycans; PQSs, putative quadruplex sequences; PTH, parathyroid hormone; qPCR, quantitative PCR; SPD, spermidine; TmPyP4, α,β,γ,δ-Tetrakis(1-methylpyridinium-4-yl)porphyrin *p*-toluenesulfonate; UST, chondroitin uronyl 2-*O*-sulfotransferase; Xyl, xylose.

Author Contribution

K.H. and T.T. designed the study. K.H., K.Y., K.A., R.J.L., K.I. and T.T. wrote the manuscript. K.Y., K.A., M.I., T.F. and K.H. conducted the cell culture, Western blotting, real-time PCR and HPLC. G.K. analyzed RNA structure by NMR. T.S. analyzed melting temperature of RNA. All authors analyzed the results and approved the final version of the manuscript.

Funding

This work was supported, in part, by the Grant-in-Aid for Young Scientists B 25870126 (to K.H.) and Grant-in-Aid for Scientific Research C 24590046 (to T.T.) and the Sasakawa Scientific Research Grant from The Japan Science Society to K.H. and Seed Grant Competition 2013 to K.H.

Acknowledgements

We thank Maina Otsu and Junpei Sahara for assistance NMR measurement. We also thank Drs N. Murai, Y. Fukumoto, H. Nakamura and H. Kitagawa for kind supply of cell lines.

PORTLAND PRESS

Competing Interests

The Authors declare that there are no competing interests associated with the manuscript.

References

1 Roden, L. (1980) Structure and metabolism of connective tissue proteoglycans. In *The Biochemistry of Glycoproteins and Proteoglycnas*, pp. 267–371, Plenum Publishing Corp., New York
2 Higashi, K., Okamoto, Y., Mano, T., Wada, T. and Toida, T. (2014) A simple HPLC method for identification of the origin of chondroitin sulfate in health food. *Jpn J. Food Chem. Safety* **21**, 187–194 https://doi.org/10.18891/jjfcs.21.3_187
3 Mizumoto, S., Yamada, S. and Sugahara, K. (2015) Molecular interactions between chondroitin-dermatan sulfate and growth factors/receptors/matrix proteins. *Curr. Opin. Struct. Biol.* **34**, 35–42 https://doi.org/10.1016/j.sbi.2015.06.004
4 Maeda, N. (2015) Proteoglycans and neuronal migration in the cerebral cortex during development and disease. *Front. Neurosci.* **9**, 98 https://doi.org/10.3389/fnins.2015.00098
5 Nairn, A.V., Kinoshita-Toyoda, A., Toyoda, H., Xie, J., Harris, K., Dalton, S. et al. (2007) Glycomics of proteoglycan biosynthesis in murine embryonic stem cell differentiation. *J. Proteome Res.* **6**, 4374–4387 https://doi.org/10.1021/pr070446f
6 Malmström, A., Bartolini, B., Thelin, M.A., Pacheco, B. and Maccarana, M. (2012) Iduronic acid in chondroitin/dermatan sulfate: biosynthesis and biological function. *J. Histochem. Cytochem.* **60**, 916–925 https://doi.org/10.1369/0022155412459857
7 Esko, J.D., Prestegard, J. and Linhardt, R.J. (2017) Proteins that bind sulfated glycosaminoglycans. In *Essentials of Glycobiology*, 3rd edn, Chapter 38, Cold Spring Harbor, New York
8 Li, G., Li, L., Tian, F., Zhang, L., Xue, C. and Linhardt, R.J. (2015) Glycosaminoglycanomics of cultured cells using a rapid and sensitive LC-MS/MS approach. *ACS Chem. Biol.* **10**, 1303–1310 https://doi.org/10.1021/acschembio.5b00011
9 Ly, M., Leach, F.E., Laremore, T.N., Toida, T., Amster, I.J. and Linhardt, R.J. (2011) The proteoglycan bikunin has a defined sequence. *Nat. Chem. Biol.* **7**, 827–833 https://doi.org/10.1038/nchembio.673
10 Yu, Y., Duan, J., Leach, F.E., Toida, T., Higashi, K., Zhang, H. et al. (2017) Sequencing the dermatan sulfate chain of decorin. *J. Am. Chem. Soc.* **139**, 16986–16995 https://doi.org/10.1021/jacs.7b10164
11 Bao, X., Nishimura, S., Mikami, T., Yamada, S., Itoh, N. and Sugahara, K. (2004) Chondroitin sulfate/dermatan sulfate hybrid chains from embryonic pig brain, which contain a higher proportion of L-iduronic acid than those from adult pig brain, exhibit neuritogenic and growth factor binding activities. *J. Biol. Chem.* **279**, 9765–9776 https://doi.org/10.1074/jbc.M310877200
12 Mizumoto, S., Ikegawa, S. and Sugahara, K. (2013) Human genetic disorders caused by mutations in genes encoding biosynthetic enzymes for sulfated glycosaminoglycans. *J. Biol. Chem.* **288**, 10953–10961 https://doi.org/10.1074/jbc.R112.437038
13 Mizumoto, S., Yamada, S. and Sugahara, K. (2014) Human genetic disorders and knockout mice deficient in glycosaminoglycan. *Biomed. Res. Int.* **2014**, 495764 https://doi.org/10.1155/2014/495764
14 Miyata, S., Komatsu, Y., Yoshimura, Y., Taya, C. and Kitagawa, H. (2012) Persistent cortical plasticity by upregulation of chondroitin 6-sulfation. *Nat. Neurosci.* **15**, 414–422, S411–412 https://doi.org/10.1038/nn.3023
15 Carrino, D.A., Calabro, A., Darr, A.B., Dours-Zimmermann, M.T., Sandy, J.D., Zimmermann, D.R. et al. (2011) Age-related differences in human skin proteoglycans. *Glycobiology* **21**, 257–268 https://doi.org/10.1093/glycob/cwq162
16 Bayliss, M.T., Osborne, D., Woodhouse, S. and Davidson, C. (1999) Sulfation of chondroitin sulfate in human articular cartilage. The effect of age, topographical position, and zone of cartilage on tissue composition. *J. Biol. Chem.* **274**, 15892–15900 https://doi.org/10.1074/jbc.274.22.15892
17 Mathews, M.B. and Glagov, S. (1966) Acid mucopolysaccharide patterns in aging human cartilage. *J. Clin. Invest.* **45**, 1103–1111 https://doi.org/10.1172/JCI105416
18 Kitagawa, H., Tsutsumi, K., Tone, Y. and Sugahara, K. (1997) Developmental regulation of the sulfation profile of chondroitin sulfate chains in the chicken embryo brain. *J. Biol. Chem.* **272**, 31377–31381 https://doi.org/10.1074/jbc.272.50.31377
19 Igarashi, K. and Kashiwagi, K. (2010) Modulation of cellular function by polyamines. *Int. J. Biochem. Cell Biol.* **42**, 39–51 https://doi.org/10.1016/j.biocel.2009.07.009
20 Watanabe, S., Kusama-Eguchi, K., Kobayashi, H. and Igarashi, K. (1991) Estimation of polyamine binding to macromolecules and ATP in bovine lymphocytes and rat liver. *J. Biol. Chem.* **266**, 20803–20809 PMID:1718969
21 Igarashi, K. and Kashiwagi, K. (2015) Modulation of protein synthesis by polyamines. *IUBMB Life* **67**, 160–169 https://doi.org/10.1002/iub.1363
22 Takigawa, M., Ishida, H., Takano, T. and Suzuki, F. (1980) Polyamine and differentiation: induction of ornithine decarboxylase by parathyroid hormone is a good marker of differentiated chondrocytes. *Proc. Natl Acad. Sci. U.S.A.* **77**, 1481–1485 https://doi.org/10.1073/pnas.77.3.1481
23 Takano, T., Takigawa, M. and Suzuki, F. (1983) Role of polyamines in expression of the differentiated phenotype of chondrocytes: effect of DL-α-hydrazino-δ-aminovaleric acid (DL-HAVA), an inhibitor of ornithine decarboxylase, on chondrocytes treated with parathyroid hormone. *J. Biochem.* **93**, 591–598 https://doi.org/10.1093/oxfordjournals.jbchem.a134214
24 Takano, T., Takigawa, M., Shirai, E., Nakagawa, K., Sakuda, M. and Suzuki, F. (1987) The effect of parathyroid hormone (1–34) on cyclic AMP level, ornithine decarboxylase activity, and glycosaminoglycan synthesis of chondrocytes from mandibular condylar cartilage, nasal septal cartilage, and spheno-occipital synchondrosis in culture. *J. Dent. Res.* **66**, 84–87 https://doi.org/10.1177/00220345870660011801
25 Nishimura, K., Shiina, R., Kashiwagi, K. and Igarashi, K. (2006) Decrease in polyamines with aging and their ingestion from food and drink. *J. Biochem.* **139**, 81–90 https://doi.org/10.1093/jb/mvj003
26 Imamura, M., Higashi, K., Yamaguchi, K., Asakura, K., Furihata, T., Terui, Y. et al. (2016) Polyamines release the let-7b-mediated suppression of initiation codon recognition during the protein synthesis of EXT2. *Sci. Rep.* **6**, 33549 https://doi.org/10.1038/srep33549
27 Lowry, O.H., Rosebrough, N.J., Farr, A.L. and Randall, R.J. (1951) Protein measurement with the Folin phenol reagent. *J. Biol. Chem.* **193**, 265–275 PMID:14907713
28 Nielsen, P.J., Manchester, K.L., Towbin, H., Gordon, J. and Thomas, G. (1982) The phosphorylation of ribosomal protein S6 in rat tissues following cycloheximide injection, in diabetes, and after denervation of diaphragm. A simple immunological determination of the extent of S6 phosphorylation on protein blots. *J. Biol. Chem.* **257**, 12316–12321 PMID:6749858

Biochemical Journal (2018) **475** 3797–3812
https://doi.org/10.1042/BCJ20180672

29 Fukumoto, Y., Obata, Y., Ishibashi, K., Tamura, N., Kikuchi, I., Aoyama, K. et al. (2010) Cost-effective gene transfection by DNA compaction at pH 4.0 using acidified, long shelf-life polyethylenimine. *Cytotechnology* **62**, 73–82 https://doi.org/10.1007/s10616-010-9259-z

30 Mémin, E., Hoque, M., Jain, M.R., Heller, D.S., Li, H., Cracchiolo, B. et al. (2014) Blocking eIF5A modification in cervical cancer cells alters the expression of cancer-related genes and suppresses cell proliferation. *Cancer Res.* **74**, 552–562 https://doi.org/10.1158/0008-5472.CAN-13-0474

31 Choe, J., Ryu, I., Park, O.H., Park, J., Cho, H., Yoo, J.S. et al. (2014) eIF4AIII enhances translation of nuclear cap-binding complex-bound mRNAs by promoting disruption of secondary structures in 5′-UTR. *Proc. Natl Acad. Sci. U.S.A.* **111**, E4577–E4586 https://doi.org/10.1073/pnas.1409695111

32 Jakus, J., Wolff, E.C., Park, M.H. and Folk, J.E. (1993) Features of the spermidine-binding site of deoxyhypusine synthase as derived from inhibition studies. Effective inhibition by bis- and mono-guanylated diamines and polyamines. *J. Biol. Chem.* **268**, 13151–13159 PMID:8514754

33 Fay, M.M., Lyons, S.M. and Ivanov, P. (2017) RNA G-quadruplexes in biology: principles and molecular mechanisms. *J. Mol. Biol.* **429**, 2127–2147 https://doi.org/10.1016/j.jmb.2017.05.017

34 Song, J., Perreault, J.P., Topisirovic, I. and Richard, S. (2016) RNA G-quadruplexes and their potential regulatory roles in translation. *Translation* **4**, e1244031 https://doi.org/10.1080/21690731.2016.1244031

35 Bugaut, A. and Balasubramanian, S. (2012) 5′-UTR RNA G-quadruplexes: translation regulation and targeting. *Nucleic Acids Res.* **40**, 4727–4741 https://doi.org/10.1093/nar/gks068

36 Kumari, S., Bugaut, A., Huppert, J.L. and Balasubramanian, S. (2007) An RNA G-quadruplex in the 5′ UTR of the NRAS proto-oncogene modulates translation. *Nat. Chem. Biol.* **3**, 218–221 https://doi.org/10.1038/nchembio864

37 Balkwill, G.D., Derecka, K., Garner, T.P., Hodgman, C., Flint, A.P. and Searle, M.S. (2009) Repression of translation of human estrogen receptor α by G-quadruplex formation. *Biochemistry* **48**, 11487–11495 https://doi.org/10.1021/bi901420k

38 Morris, M.J. and Basu, S. (2009) An unusually stable G-quadruplex within the 5′-UTR of the MT3 matrix metalloproteinase mRNA represses translation in eukaryotic cells. *Biochemistry* **48**, 5313–5319 https://doi.org/10.1021/bi900498z

39 Shahid, R., Bugaut, A. and Balasubramanian, S. (2010) The *BCL-2* 5′ untranslated region contains an RNA G-quadruplex-forming motif that modulates protein expression. *Biochemistry* **49**, 8300–8306 https://doi.org/10.1021/bi100957h

40 Gomez, D., Guédin, A., Mergny, J.-L., Salles, B., Riou, J.-F., Teulade-Fichou, M.-P. et al. (2010) A G-quadruplex structure within the 5′-UTR of TRF2 mRNA represses translation in human cells. *Nucleic Acids Res.* **38**, 7187–7198 https://doi.org/10.1093/nar/gkq563

41 Lammich, S., Kamp, F., Wagner, J., Nuscher, B., Zilow, S., Ludwig, A.-K. et al. (2011) Translational repression of the disintegrin and metalloprotease ADAM10 by a stable G-quadruplex secondary structure in its 5′-untranslated region. *J. Biol. Chem.* **286**, 45063–45072 https://doi.org/10.1074/jbc.M111.296921

42 Beaudoin, J.-D., Jodoin, R. and Perreault, J.-P. (2014) New scoring system to identify RNA G-quadruplex folding. *Nucleic Acids Res.* **42**, 1209–1223 https://doi.org/10.1093/nar/gkt904

43 Wolfe, A.L., Singh, K., Zhong, Y., Drewe, P., Rajasekhar, V.K., Sanghvi, V.R. et al. (2014) RNA G-quadruplexes cause eIF4A-dependent oncogene translation in cancer. *Nature* **513**, 65–70 https://doi.org/10.1038/nature13485

44 Malgowska, M., Gudanis, D., Kierzek, R., Wyszko, E., Gabelica, V. and Gdaniec, Z. (2014) Distinctive structural motifs of RNA G-quadruplexes composed of AGG, CGG and UGG trinucleotide repeats. *Nucleic Acids Res.* **42**, 10196–10207 https://doi.org/10.1093/nar/gku710

45 Lyons, S.M., Gudanis, D., Coyne, S.M., Gdaniec, Z. and Ivanov, P. (2017) Identification of functional tetramolecular RNA G-quadruplexes derived from transfer RNAs. *Nat. Commun.* **8**, 1127 https://doi.org/10.1038/s41467-017-01278-w

46 Siddiqui-Jain, A., Grand, C.L., Bearss, D.J. and Hurley, L.H. (2002) Direct evidence for a G-quadruplex in a promoter region and its targeting with a small molecule to repress c-MYC transcription. *Proc. Natl Acad. Sci. U.S.A.* **99**, 11593–11598 https://doi.org/10.1073/pnas.182256799

47 Morris, M.J., Wingate, K.L., Silwal, J., Leeper, T.C. and Basu, S. (2012) The porphyrin TmPyP4 unfolds the extremely stable G-quadruplex in MT3-MMP mRNA and alleviates its repressive effect to enhance translation in eukaryotic cells. *Nucleic Acids Res.* **40**, 4137–4145 https://doi.org/10.1093/nar/gkr1308

48 von Hacht, A., Seifert, O., Menger, M., Schütze, T., Arora, A., Konthur, Z. et al. (2014) Identification and characterization of RNA guanine-quadruplex binding proteins. *Nucleic Acids Res.* **42**, 6630–6644 https://doi.org/10.1093/nar/gku290

49 Thandapani, P., Song, J., Gandin, V., Cai, Y., Rouleau, S.G., Garant, J.-M. et al. (2015) Aven recognition of RNA G-quadruplexes regulates translation of the mixed lineage leukemia protooncogenes. *eLife* **4**, e06234 https://doi.org/10.7554/eLife.06234

50 McRae, E.K.S., Booy, E.P., Moya-Torres, A., Ezzati, P., Stetefeld, J. and McKenna, S.A. (2017) Human DDX21 binds and unwinds RNA guanine quadruplexes. *Nucleic Acids Res.* **45**, 6656–6668 https://doi.org/10.1093/nar/gkx380

51 Benhalevy, D., Gupta, S.K., Danan, C.H., Ghosal, S., Sun, H.-W., Kazemier, H.G. et al. (2017) The human CCHC-type zinc finger nucleic acid-binding protein binds G-rich elements in target mRNA coding sequences and promotes translation. *Cell Rep.* **18**, 2979–2990 https://doi.org/10.1016/j.celrep.2017.02.080

52 Izumikawa, T., Koike, T., Shiozawa, S., Sugahara, K., Tamura, J. and Kitagawa, H. (2008) Identification of chondroitin sulfate glucuronyltransferase as chondroitin synthase-3 involved in chondroitin polymerization: chondroitin polymerization is achieved by multiple enzyme complexes consisting of chondroitin synthase family members. *J. Biol. Chem.* **283**, 11396–11406 https://doi.org/10.1074/jbc.M707549200

53 Izumikawa, T., Koike, T. and Kitagawa, H. (2012) Chondroitin 4-*O*-sulfotransferase-2 regulates the number of chondroitin sulfate chains initiated by chondroitin *N*-acetylgalactosaminyltransferase-1. *Biochem. J.* **441**, 697–705 https://doi.org/10.1042/BJ20111472